

## Supporting Information

### Ink-Lithography for Property Engineering and Patterning of Nanocrystal Thin Films

Junhyuk Ahn<sup>1</sup>, Sanghyun Jeon<sup>1</sup>, Ho Kun Woo<sup>1</sup>, Junsung Bang<sup>1</sup>, Yong Min Lee<sup>2</sup>, Steven J. Neuhaus<sup>4</sup>, Woo Seok Lee<sup>1</sup>, Taesung Park<sup>1</sup>, Sang Yeop Lee<sup>1</sup>, Byung Ku Jung<sup>1</sup>, Hyungmok Joh<sup>1</sup>, Mingi Seong<sup>1</sup>, Ji-hyuk Choi<sup>6</sup>, Ho Gyu Yoon<sup>1</sup>, Cherie R. Kagan<sup>3,4,5\*</sup> and Soong Ju Oh<sup>1\*</sup>

**Materials.** Cadmium oxide (CdO, >99.5 %, powder), selenium (Se, metal basis), diphenylphosphine (DPP, >95 %), octadecylamine (>99.0 %), oleic acid (OA, tech., 90 %), oleylamine (OAm, 70 %), tetrabutylammonium bromide (TBAB, ACS reagent), 3-mercaptopropionic acid (MPA, >99 %), indium (III) chloride (95 %), lead (II) bromide (>98 %), lead (II) oxide (99.999 % trace metals basis), trioctylamine (TOA, 95 %), 1-octadecene (ODE, 90 %), and zinc acetate dihydrate (ACS reagent, >98%) were purchased from Sigma-Aldrich. Silver nitrate (AgNO<sub>3</sub>, ACS, >99.9 %, metal basis), and tetra-*n*-butylammonium iodide (TBAI, 98 %), sodium iodide (NaI, >99+ % dry weight, water), tetramethylammonium hydroxide (TMAOH, 25 % w/w in methanol), cesium bromide (CsBr, 99.999 %, metal basis), and dimethyl sulfoxide (DMSO, anhydrous, 99.8 %) were purchased from Alfa Aesar. Toluene (99.5 %), ethanol (EtOH, 95.0 %), methyl alcohol (MeOH, 99.5 %), acetone (99.5 %), potassium hydroxide (KOH, 95.0 %), and isopropanol (IPA, 99.5 %) were purchased from Samchun Chemicals. Ammonium bromide (NH<sub>4</sub>Br, ACS Reagent >99.0 %) ammonium iodide (NH<sub>4</sub>I, ACS Reagent, 99%), and ammonium chloride (NH<sub>4</sub>Cl, ACS Reagent, >99.0 %) and ammonium thiocyanate (NH<sub>4</sub>SCN, ACS Reagent, >97.5 %) were purchased from Honeywell Fluka.

**Details of the inkjet cartridge.** The dot size is 30 μm, the number of nozzles is 12 jets, the jetting frequency for printing is 15 kHz, printing speed is 300 mm/s, and the theoretical

maximum number of pixels is 846 ppi (pixels per inch) (Dimatix Materials Cartridge – Samba Cartridge).

**Fabrication of CdSe NC-based *n*-type transistors.** Thermally oxidized (250 nm SiO<sub>2</sub>), heavily doped Si wafers are used as gate dielectric and gate layers for TFTs. 60 nm Au source and drain electrodes are deposited using a thermal evaporator through a shadow mask to define two TFTs with a channel width-to-length ratio of 15. On the prepared Si wafer coated with CdSe NC thin films, InCl<sub>3</sub> ligand ink is treated to obtain *n*-type transistors. The CdSe NC thin films are then annealed at 250 °C for 20 min.

## DISCUSSION 1 | Selection of the parent-solvent for the ligand ink

As beforementioned in this paper, the solvent for the ligand inks should meet four criteria: i) have high ligand solubility, ii) support efficient ligand exchange, iii) be printable, and iv) have a high enough contact angle on NC films. Various solvents including water, methanol (MeOH), ethanol (EtOH), *iso*-propanol (IPA), dimethylformamide (DMF), acetone, methyl acetate (M.A.), and ethylene glycol (EG) are examined (**Table S1**). Among them, M.A. provides limited ligand solubilities of less than 1 mM due to its relative low polarity. The ligand exchangeability of each solvent is examined by FTIR spectroscopy (**Figure S2**) using NH<sub>4</sub>SCN ligand salts. Only in the case of water, the C-H stretch at 2800 to 3200 cm<sup>-1</sup>, corresponding to the original ligands remains. This indicates that ligand exchange does not effectively occur when water is used as a solvent. Therefore, M.A. and water are excluded from the list of solvents further explored for the ligand inks.

Patterning performances of each solvent can be predicted using the dimensionless Weber ( $W_e$ ), Reynolds ( $R_e$ ), and Ohnesorge ( $Oh$ ) numbers.  $W_e$  is useful in analyzing a fluid's inertia and surface tension and are compared to predict the formation of droplets.  $R_e$  is a measure of fluid flow through a comparison between the inertial force and viscosity.  $Oh$  is helpful in conjecturing whether a droplet is generated or a satellite is formed by analyzing the viscosity. The value of  $Oh$  is typically described as  $Z$ , which is inversely proportional to  $Oh$  ( $Z = 1/Oh$ ). These numbers are closely related to each other and are defined as follows:

$$W_e = \frac{\rho v^2 a}{\gamma} \quad (1)$$

$$R_e = \frac{\rho v a}{\eta} \quad (2)$$

$$Oh = \frac{\sqrt{W_e}}{R_e} = \frac{\eta}{\sqrt{\gamma \rho a}} \quad (3)$$

where  $\rho$ ,  $\gamma$ ,  $a$ ,  $v$ , and  $\eta$  are the density of the fluid, the surface tension, the droplet diameter, the velocity, and the dynamic viscosity of the fluid, respectively; and  $a$  is used as the diameter of the cartridge nozzle of 21.0  $\mu\text{m}$ .

The printable fluids are compared through visualization that of results using the  $(x, y)$  coordinate of  $(R_e, W_e)$  expressed in **Figure S3**. Each value is tabulated in **Table S1**. The  $R_e$ - $W_e$  plot diagram follows that proposed by Derby, B. *et al.*<sup>1</sup> Except for the IPA solvent, the coordinates of all solvents are positioned out of printable fluid ranges. Therefore, IPA is selected as the most suitable parent-solvent for ink-lithography.

Furthermore, the dropping behavior can be readily predicted by comparing the values of  $Z$  as shown in **Table S1**. Indeed, Jang *et al.* proposed that the useful printable fluid range is  $4 < Z < 14$ .<sup>2</sup> Capillary forces suppress droplet generation when  $Z$  is lower than 4, which indicates that the solvent droplet cannot be formed and dropped from the cartridge due to its insufficient droplet formation energy. For example, ethylene glycol ( $Z$ ; 2.05) cannot be extracted from the inkjet cartridge owing to its high viscosity and surface tension. By contrast, if  $Z$  is higher than 14, satellite drops are formed due to low viscosity and high surface tension of the solvent, creating unwanted patterns. IPA solvent has a  $Z$ -value of 9.54, positioned within printable fluid ranges. Other solvents fall out of the printable range. Contact angle test shows that all solvents satisfy the wettability conditions (**Figure S4**).

With the results of the dimensionless numbers, the patterning performance of each solvent is examined by inkjet printing the ink in rectangular patterns of  $800 \times 600 \mu\text{m}^2$  on CdSe NC thin films. In **Figure S5**, IPA shows the best performance, forming patterned films near the size and shape of our target pattern area, as described in the main text.

To improve the ink-lithography performances, the coordinate of  $(R_e, W_e)$  which is expressed in **Figure S3** is adjusted by mixing additional EG into the parent IPA solvent, engineering the viscosity and surface tension of the solvent. For the mixed solvent, the coordinate is positioned by calculating characteristics of binary solvent mixture (see the calculation part). As the amount

of EG mixed in IPA increases, the coordinate of ( $R_e$ ,  $W_e$ ) is shifted to the middle of the range of printable fluids (**Table S2** and **Figure S3**). However, it is found that excessive amounts of EG degrades pattern formation as  $W_e$  drops and the ink cannot be jetted from the inkjet-cartridge owing to insufficient energy of droplet formation (**Figure S6**).

Besides understanding the dropping behavior, wettability on the ink on the NC thin film should be considered to improve pattern resolution. The spreading of the solvent on the NC thin-film surface can be explained by the polarity or surface tension of the solvent. In order to quantify the wettability of each solvent, we analyze the contact angle upon printing each solvent onto the as-synthesized, hydrophobic CdSe NC thin films. As seen in **Figure S4**, mixing EG into the IPA increases the ink polarity, changing the contact angle from  $11^\circ$  to  $18^\circ$ . As a result, it reduces the spreading effect and improves the patterning performance.

## DISCUSSION 2 | Calculation of the characteristics of the binary solvents

The dimensionless numbers of a binary solvent require the characteristics of the mixture, such as its density, kinematic viscosity, and surface tension. We obtain each characteristic through the following equations. First, the density of the binary mixture ( $D_{mix}$ ) is calculated as:<sup>3</sup>

$$D_{mix} = \frac{100}{\left(\frac{x_1}{D_1} + \frac{x_2}{D_2}\right)} \quad (4)$$

where  $x_i$  is the mass fraction and  $D_i$  is the density of components 1 or 2. It is assumed that each solvent does not show interactions upon mixing.

The kinematic viscosity ( $\nu$ ) of a mixture of two or more liquids is calculated using the Refutas method.<sup>4</sup> The viscosity blending number (VBN) of each component is used for the calculation as follows:

$$VBN_i = 14.534 \times \ln(\ln(\nu_i + 0.8)) + 10.975. \quad (5)$$

where the  $\nu_i$  is the kinematic viscosity of the component in the mixture. The VBN of the mixed solvent is then calculated as follows:

$$VBN_{mix} = \sum_{i=0}^N x_i \times VBN_i \quad (6)$$

Then, the kinematic viscosity of the binary solvent can be estimated by combining the two equations as follows:

$$\nu_{mix} = \exp\left(\exp\left(\frac{VBN_{mix} - 10.975}{14.534}\right)\right) - 0.8 \quad (7)$$

Finally, the surface tension ( $\gamma$ ) of the binary systems is calculated using the method reported by Eberhart *et al.*<sup>5</sup> The equation is expressed as follows:

$$\gamma_{mix} = \frac{D_1 V_1}{D_1 V_1 + D_2 V_2} \gamma_1 + \frac{D_2 V_2}{D_1 V_1 + D_2 V_2} \gamma_2 \quad (8)$$

where  $D$  and  $V$  are the density and volume fraction of each solvent, respectively.

According to the equations which express density, kinematic viscosity, and surface tension of the mixed solvent, we achieve characteristics of the mixed solutions and compare it to those

of the components. We then tabulate those results and corresponding value of  $W_e$ ,  $R_e$ , and  $Oh$  in **Table S2**.

## RESULTS

	Density [kg/m <sup>3</sup> ]	Viscosity [mPa s]	Surface tension [mN/m]	$N_{Re}$	$N_{We}$	$N_{Oh}$	$Z$
Water	1000	0.89	72.7	70.8	2.6	0.02	43.9
MeOH	787	0.54	22.1	91.8	6.7	0.03	35.4
EtOH	787	1.07	22.0	46.3	6.8	0.06	17.8
IPA	783	2.05	23.3	24.1	6.35	0.10	9.5
Acetone	784	0.31	23.0	159.3	6.4	0.02	62.8
DMF	945	0.79	34.4	73.4	5.2	0.03	33.1
M.A.	927	0.36	24.5	162.2	7.2	0.02	60.7
EG	1105	15.80	45.5	4.4	4.6	0.49	2.05

**Table S1.** Summary of physical properties and dimensionless numbers for different fluids (average velocity and length are 3.0 m/s and 21.0  $\mu\text{m}$ ).



Mixture	Density [kg/m <sup>3</sup> ]	Viscosity [mPa s]	Surface tension [mN/m]	$N_{Re}$	$N_{We}$	$N_{Oh}$	$Z$
0.1% EG	783.3	2.05	23.3	24.02	6.35	0.10	9.53
0.5% EG	784.6	2.07	23.5	23.88	6.31	0.11	9.51
1.0% EG	786.3	2.09	23.6	23.70	6.30	0.11	9.45
5.0% EG	799.4	2.27	24.8	22.19	6.09	0.11	8.99

**Table S2.** Summary of physical properties and dimensionless numbers for different fluids (average velocity and length are 3.0 m/s and 21.0  $\mu\text{m}$ ).

Ligand solute	$\lambda$ shift (%)	PL <sub>ligand-treated</sub> /PL <sub>as-synthesized</sub> (%)
TBAI	0.1	17.4
TBAC	0.6	11.7
NaCl	0.2	71.4
NH <sub>4</sub> Cl	2.6	16.5
CsCl	0.2	90.0
InCl <sub>3</sub>	1.9	1.5
MPA	0.2	90.3
NH <sub>4</sub> SCN	0.9	10.1
PbAc <sub>2</sub>	0.2	147.3
ZnAc <sub>2</sub>	0	45.5
PVP	-0.1	62.6
Ascorbic acid	-0.7	47.1
TDDPA	0.6	9.6
Hexadecylamine	0	30.1
1-ocadecanol	0.2	23.7

**Table S3.** Comparison of PL wavelength and intensity for different ligand ink treatments, relative to as-synthesized CdSe NC thin films.

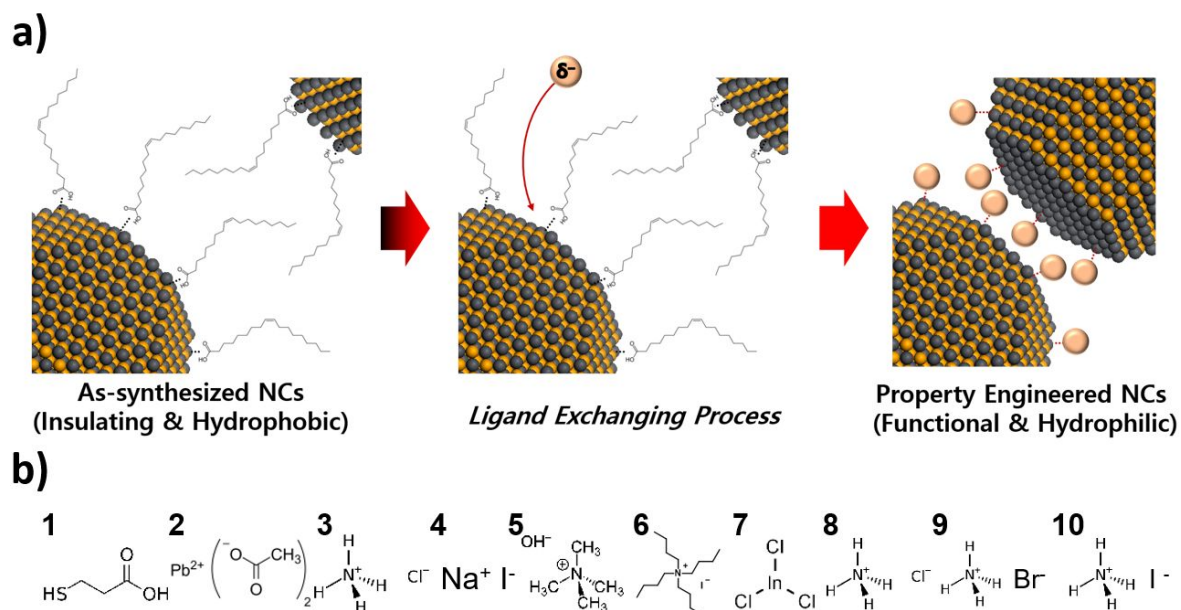


**Figure S1.** (a) Schematic of the ligand exchange process: foreign molecules with higher ligand affinity and excess volume of ligands can induce ligand exchange. (b) Candidate functional ligand inks: (1, 2) luminescence maintainer/enhancers, (3, 4) color changers to blue/red, (5) *p*-dopant, (6) *n*-dopant, (7) *n*-dopant and mobility enhancer, (8) conductivity enhancer, (9) temperature-sensitive ligand, and (10) strain-sensitive ligand.

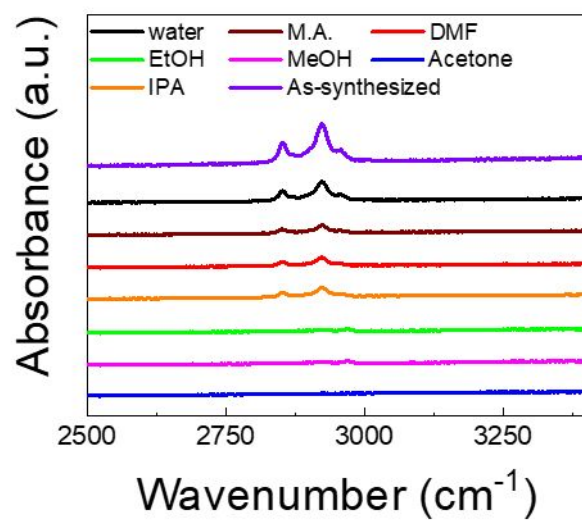


**Figure S2.** FTIR spectra of CdSe NC thin films treated with NH<sub>4</sub>SCN in various solvents and as-synthesized CdSe NC thin films.

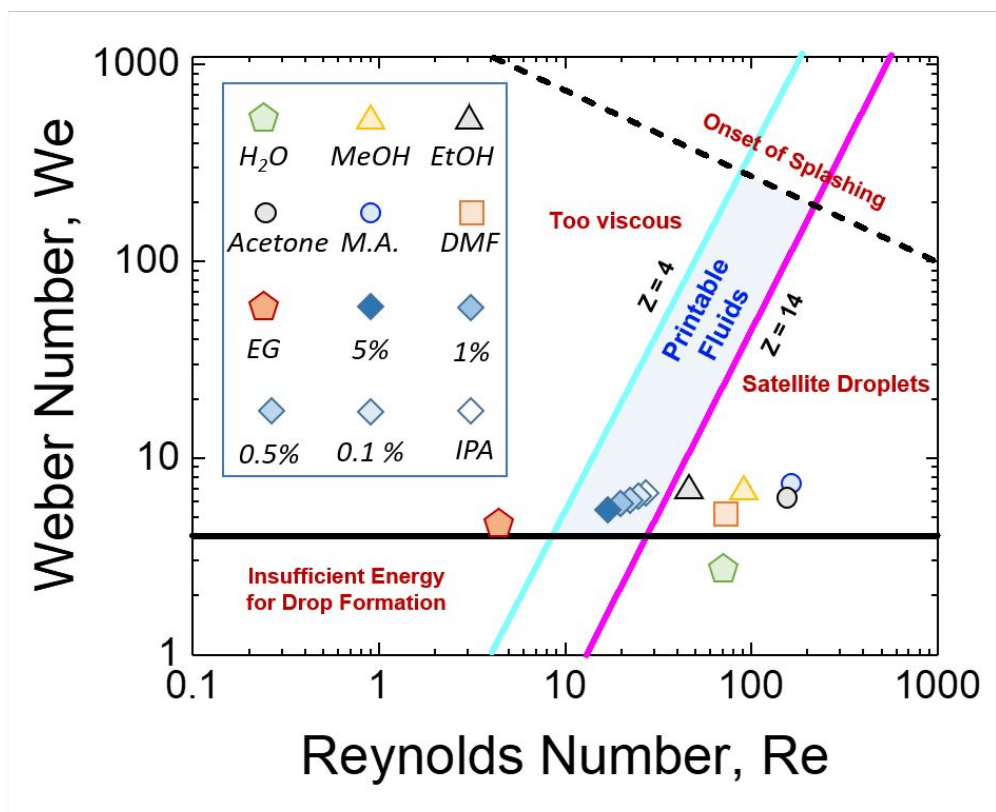


**Figure S3.**  $Re$ - $We$  plot of ligand-ink candidates for inkjet printing summarized in Tables S1-S2. Cyan and magenta line represent borderline printable fluids ( $4 < Z < 14$ ). The schematic follows the schematic diagram of Derby *et al.*<sup>1,2</sup>

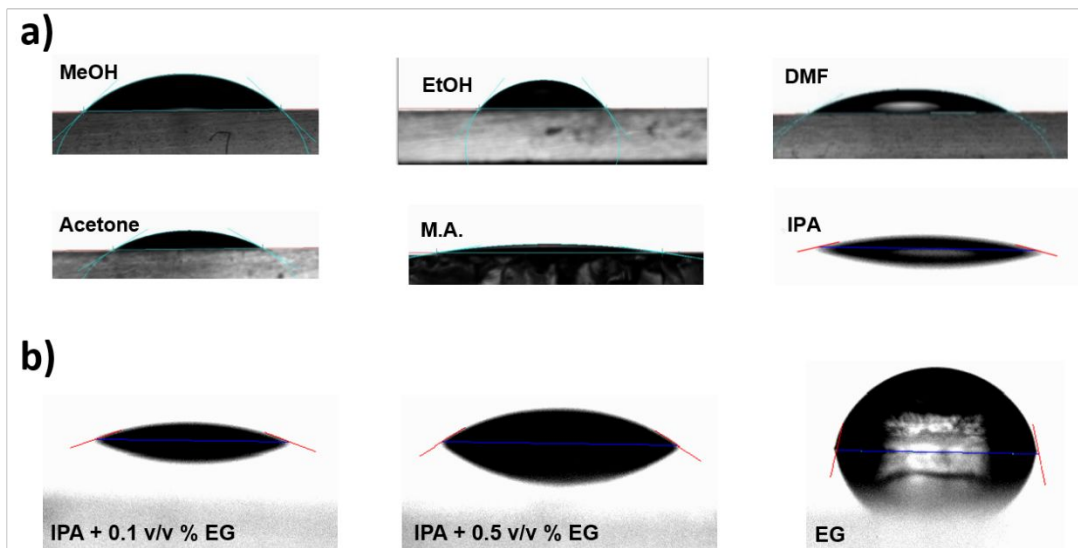


**Figure S4.** Contact angle images of droplets of (a) MeOH (43.8°), EtOH (53.8°), DMF (10.3°), acetone (30.4°), M.A. (9.0°), and IPA (11.3°) on as-synthesized CdSe NC thin films and of (b) IPA + 0.1 (13.1°), 0.5 (17.8°), and 100 v/v % EG (79.0°) on as-synthesized CdSe NC thin films.

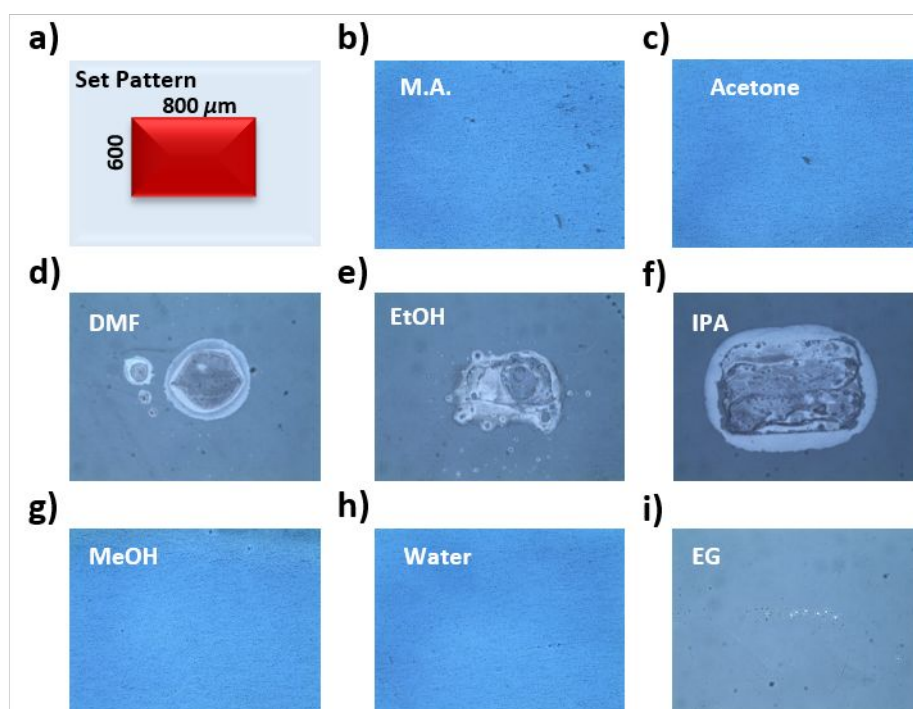


**Figure S5.** (a) Schematic of the target, inkjet printed rectangular pattern ( $800\ \mu\text{m} \times 600\ \mu\text{m}$ ). Optical images of CdSe NC films treated in the rectangular pattern through inkjetting of a  $\text{NH}_4\text{SCN}$  ligand ink in various solvents: (b) M.A., (c) acetone, (d) DMF, (e) EtOH, (f) IPA, (g) MeOH, (h) water, and (i) EG.

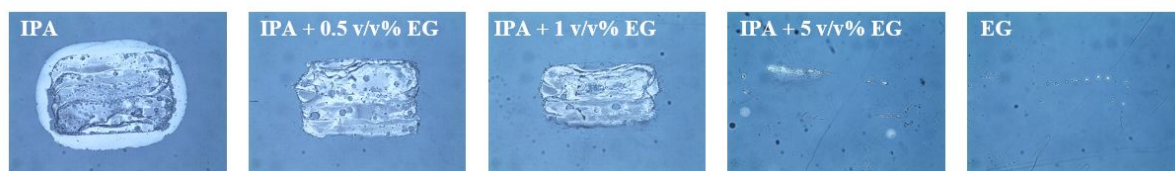


**Figure S6.** Optical images of CdSe NC films treated in a rectangular pattern of  $800\ \mu\text{m} \times 600\ \mu\text{m}$  using inkjetting of an  $\text{NH}_4\text{SCN}$  ligand ink having mixed solvents with a volume ratio of EG in IPA of 0, 0.5, 1, 5, and 100 v/v %.



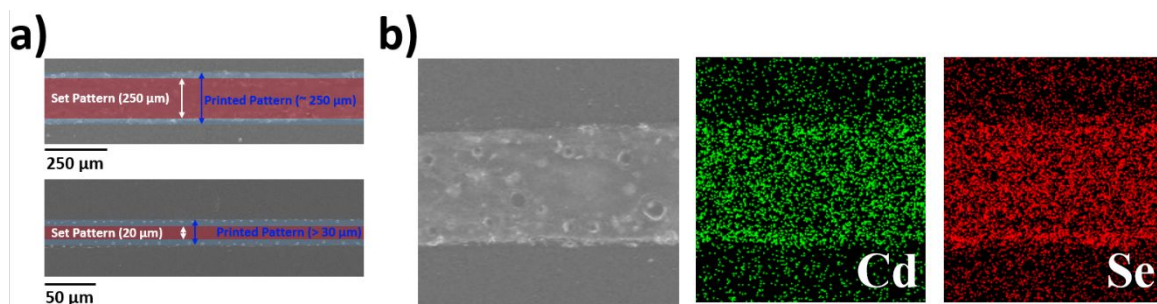


**Figure S7.** (a) SEM images of the line patterns of large (upper; target size = 250  $\mu\text{m}$  and printed size = 261  $\mu\text{m}$ ) and small (lower; target size = 20  $\mu\text{m}$  and printed size = 56  $\mu\text{m}$ ) patterns (red band = preset pattern, blue = printed pattern). (b) SEM image (left) and EDX maps of Cd (middle, green) and Se (right, red) for CdSe NC line patterns fabricated using inkjetting of  $\text{NH}_4\text{SCN}$  ligand ink.



**Figure S8.** Photograph of hand-printed letters reading “Ag NCs” on a glass bottle with Ag NC thin films treated with an  $\text{NH}_4\text{Br}$  ligand ink.

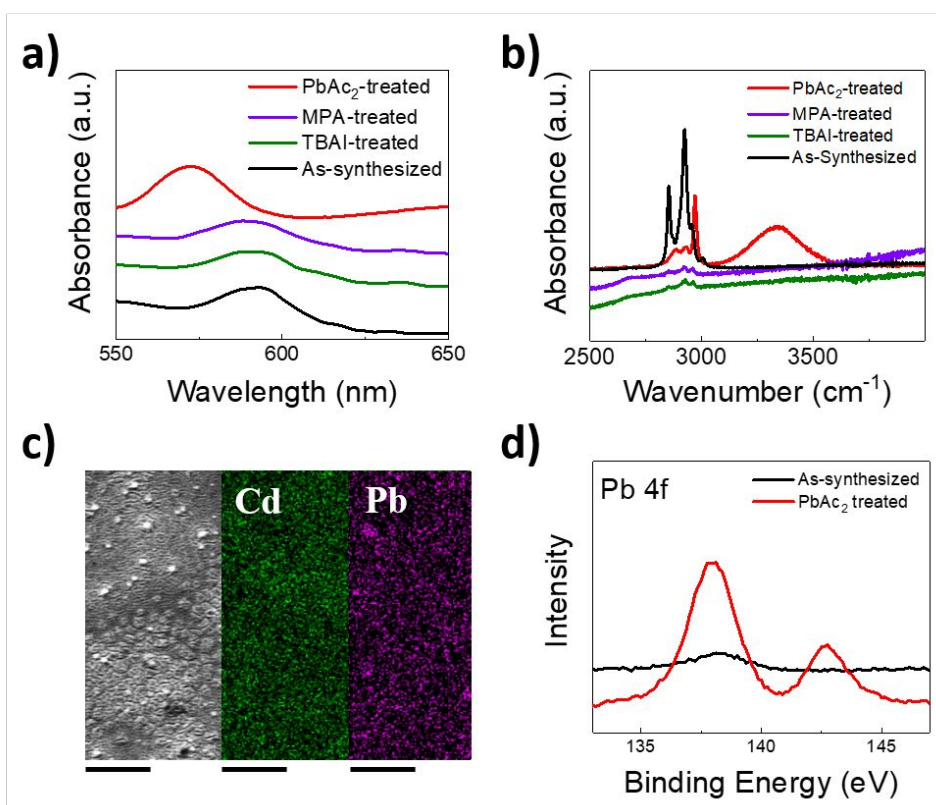


**Figure S9.** (a) Absorption spectra and (b) FTIR spectra for as-synthesized (black), TBAI-treated (dark green), MPA-treated (purple), and PbAc<sub>2</sub>-treated (red) CdSe NC thin films (-OH group fingerprint at 3395–3410 cm<sup>-1</sup>). (c) SEM image and EDX maps (green = Cd element and purple = Pb element) of PbAc<sub>2</sub>-treated CdSe NC thin films (scale bar = 25 μm), (d) XPS spectrum of PbAc<sub>2</sub>-treated CdSe NC thin films.



**Figure S10.** Optical image of negative PL patterning of the logo of “*Korea University*” by inkjetting a TBAI ligand ink onto CdSe NC thin films (scale bar = 5 mm) (Logo printed with permission from Korea University).

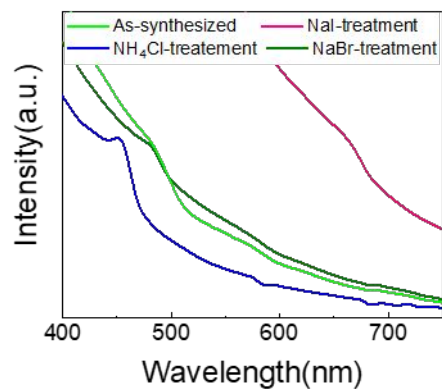


**Figure S11.** UV-Vis spectrum of as-synthesized (green), NaI- (red), NH<sub>4</sub>Cl- (blue), and NaBr-treated (dark green) CsPbBr<sub>3</sub> perovskite NC thin films.

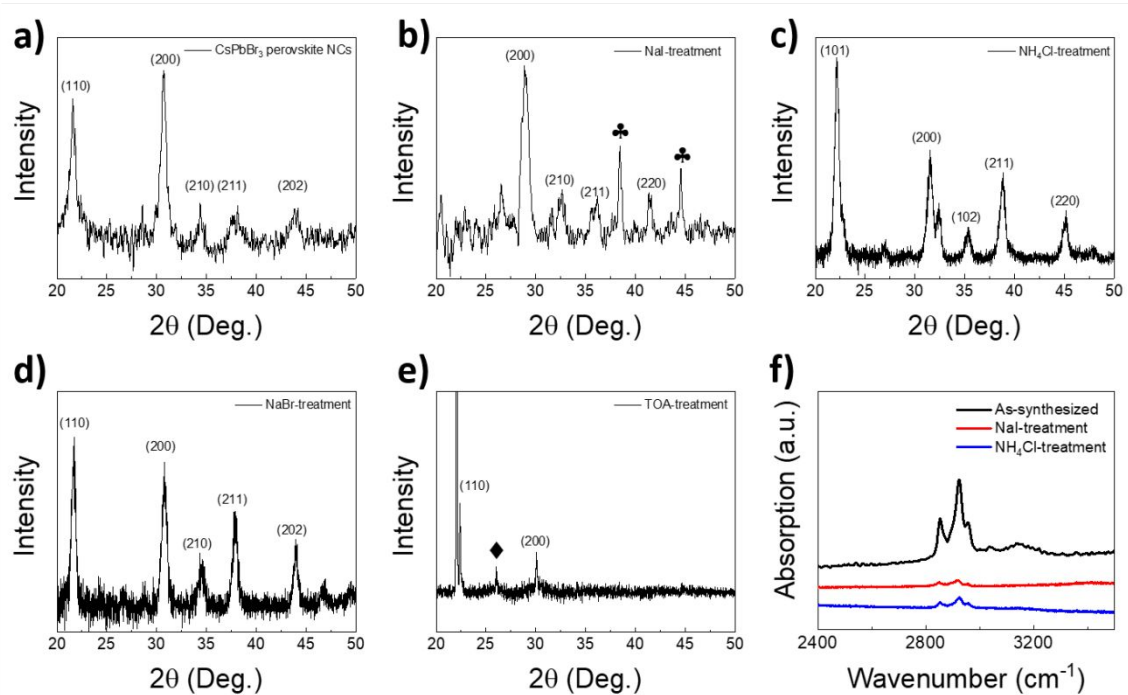


**Figure S12.** XRD spectra of cubic phase (a) as-synthesized, (b) NaI-treated ( $\clubsuit$  = peak of orthorhombic phase of  $\text{CsPbI}_3$ ), (c)  $\text{NH}_4\text{Cl}$ -treated, (d) NaBr-treated, and (e) TOA-treated  $\text{CsPbBr}_3$  perovskite NCs. (f) FTIR spectra of as-synthesized (black) and NaI- (red) and  $\text{NH}_4\text{Cl}$ - (blue) treated  $\text{CsPbBr}_3$  perovskite NC thin films.

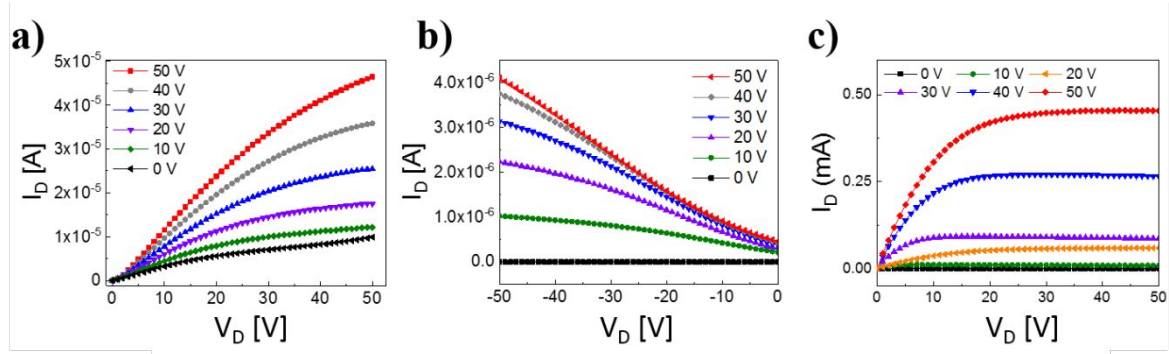


**Figure S13.** Output curves of (a) TBAI-treated PbSe NC, (b) TMAOH-treated PbSe NC, and (c) InCl<sub>3</sub>-treated CdSe NC TFTs gate voltages ranging from  $V_G=0$  V to 50 V.

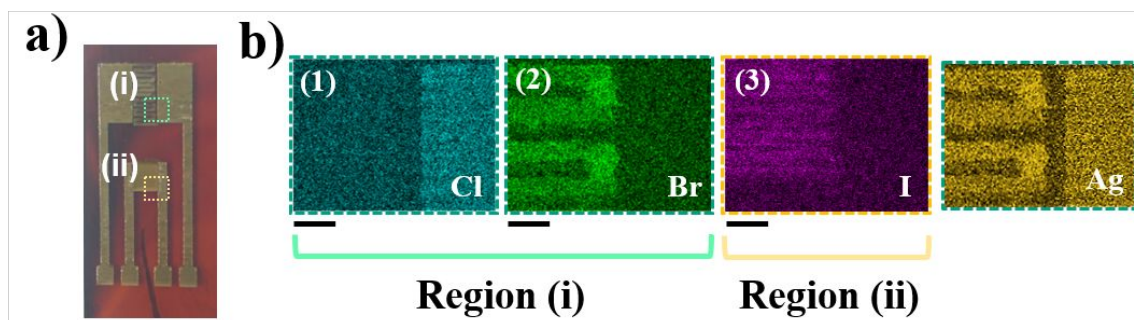


**Figure S14.** (a) Images of multi-functional sensors composed of Ag NC thin films. (b) EDX map of Cl (left) and Br (middle) elements obtained from the green box highlighting region (i), and of I (right) obtained from the yellow box highlighting region (ii) of Figure 5b (scale bar = 500  $\mu\text{m}$ ). EDX map of Ag (right).



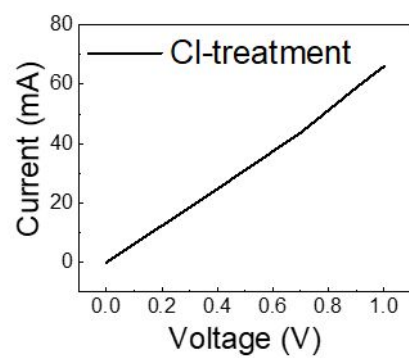


**Figure S15.** I-V curve of Cl-treated Ag NC thin films using inkjet printing.

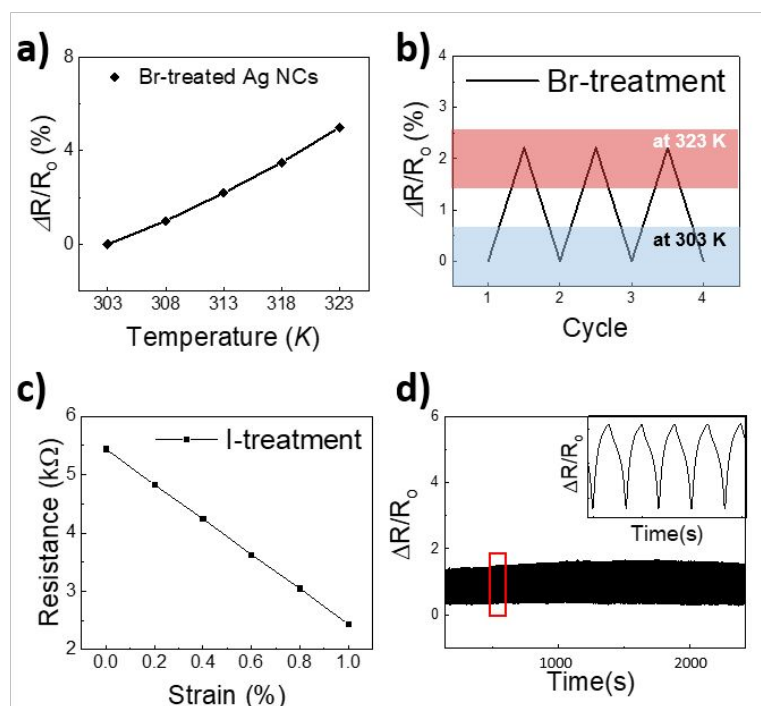


**Figure S16.** (a) Resistance of Br-treated Ag NC thin films as a function of temperature and (b) thermal cycle test of the Br-treated Ag NC thin films. (c) Resistance of I-treated Ag NC thin films as a function of strain and (d) strain cycle test of I-treated Ag NC thin films (inset = enlarged data of red box of the cycle test).

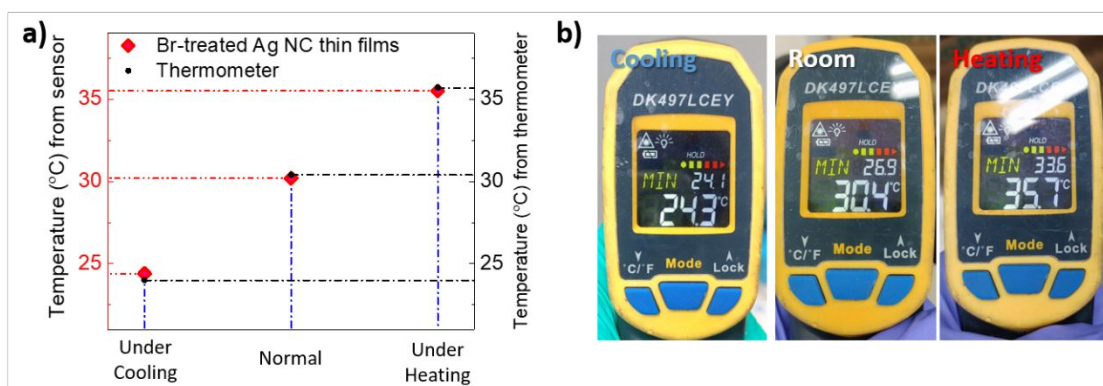


**Figure S17.** (a) Temperature measurements calculated from resistance changes in Br-treated Ag NC thin films (red diamond) and collected with a commercial thermometer (black circle). (b) Optical images of commercial thermometer displaying the measured temperatures.

## Reference

- (1) Rho, Y.; Kang, K. -T.; Lee, D. Highly Crystalline Ni/NiO Hybrid Electrodes Processed by Inkjet Printing and Laser-Induced Reductive Sintering under Ambient Conditions. *Nanoscale* **2016**, *8*, 8976–8985.
- (2) Jang, D.; Kim, D.; Moon, J. Influence of Fluid Physical Properties on Ink-Jet Printability. *Langmuir* **2009**, *25*, 2629–2635.
- (3) Feinstein, H. I. Density of a Binary Mixture: A Classroom or Laboratory Exercise. *J. Chem. Educ.* **1970**, *49*, 22030.
- (4) Zhmud, B. Viscosity Blending Equations. *Lube Mag.* **2014**, *93*, 2–5.